05,11

Magnetocaloric features of the $NiMn_{1-x}Cr_xGe$ system due to the diffuse nature of the first-order structural transitions $P6_3/mmc \leftrightarrow Pnma$

© V.I. Valkov[1], A.V. Golovchan[1], I.F. Gribanov[1], O.E. Kovalev[1], V.I. Mitsiuk[2]

[1] Donetsk Institute of Physics and Technology named after. A.A. Galkina, Donetsk, Russia
[2] Scientific Practical Materials Research Centre of NAS of Belarus, Minsk, Belarus

E-mail: valkov09@gmail.com

Received March 18, 2024
Revised May 13, 2024
Accepted May 21, 2024

An approach is proposed to describe the magnetostructural features of the $Mn_{1-x}Cr_xNiGe$ system within the concept of diffuse first-order phase transitions. The approach is based on the combination of two models for describing first-order structural transitions $\mathrm{hex}(P6_3/mmc) \leftrightarrow \mathrm{orth}(Pnma)$. The microscopic model of first-order point transitions is used to describe the phase state of a homogeneous medium of an orthorhombic phase nucleus. The thermodynamic model of redistribution of nuclei of both phases of a heterogeneous medium of a sample under the action of the entropy of mixing is used to describe the macroscopic phase state. Within the framework of the model used, an explanation is given for three types of phase transitions observed in systems with structural instability. It is shown that the reversible and first-order magnetostructural transitions observed in samples $x = 0.18$, $x = 0.25$, respectively, can be realized in sample $x = 0.11$ with an isostructural second-order magnetic transition when the sample is subjected to hydrostatic pressure.

Keywords: diffuse structural phase transitions, diffuse magnetostructural 1-st order phase transitions, heterogeneous medium, helimagnetism.

DOI: 10.61011/PSS.2024.06.58711.68

1. Introduction

Structural transitions from the hexagonal $\mathrm{hex}(P6_3/mmc)$ to the orthorhombic $\mathrm{orth}(Pnma)$ state in the paramagnetic (PM) temperature range $\mathrm{PMhex}(P6_3/mmc) \leftrightarrow \mathrm{PMorth}(Pnma)$ of the $Mn_{1-x}Cr_xNiGe$ system have a number of characteristics that allow them to be classified as structural phase transitions 1-st order. Such characteristics include a significant change in specific volume, spontaneous release (absorption) of heat and large temperature hysteresis [1]. However, since these characteristics are not realized abruptly (which, according to Ehrenfest, is a required condition [2]), these transitions can be classified as smeared phase transitions of the 1-st order [3–6]. One of the indicators of the smearing of the structural transition $\mathrm{PMhex}(P6_3/mmc) \leftrightarrow \mathrm{PMorth}(Pnma)$ is a smooth change in the content of the orthorhombic phase $Pnma$ in the sample $\text{X-Int}_{\mathrm{orth}}(T)$ within a finite range of characteristic transition temperatures. The temperature dependence of $\text{X-Int}_{\mathrm{orth}}(T)$, Figure 1, *b*, was determined by the method of X-ray diffraction analysis from changes in the intensities of diffraction maxima of alternating phases. When the sample is heated or cooled in certain temperature intervals, there is a monotonic change in $\text{X-Int}_{\mathrm{orth}}(T)$. These temperature intervals are assumed to determine the degree of smearing of the 1-st order structural transition $\mathrm{PMhex}(P6_3/mmc) \leftrightarrow \mathrm{PMorth}(Pnma)$.

In Figure 1, the experimental dependence $\text{X-Int}_{\mathrm{orth}}(T)$ for a sample with $x = 0.11$ shows a smearing of the transition as part of $\Delta_h = 56\,\mathrm{K}$ upon heating and on the order of $\Delta_c = 65\,\mathrm{K}$ upon cooling. These quantities should approach zero and the dependences $\text{X-Int}_{\mathrm{orth}}(T)$ will be described by the step functions $L_{1c}(T) = \Phi(T_{t1} - T)$, $L_{1h}(T) = \Phi(T_{t2} - T)$, Figure 2, *b* for the model of point transition of the 1-st order. The model dependences of $\chi^{-1}(T)$ and the structural order parameter also demonstrate stepwise characteristics near the temperatures of lability (absolute instability) of homogeneous paramagnetic structural states: hexagonal $\mathrm{PMhex}(P6_3/mmc) - T_{t1}$ and orthorhombic $\mathrm{PMhex}(P6_3/mmc) - T_{t2}$. As applied to samples of the $NiMn_{1-x}Cr_xGe$ system, the model of point transitions in a homogeneous medium [7] (exchange-structural model) is given in the Appendix. In this work, the theoretical analysis of smeared structural transitions is based on a thermodynamic model of the redistribution of homogeneous particles — nuclei of structural phases. In this case, the state of the nuclei is described as part of a microscopic model of point transitions for a homogeneous medium [7]. The experimental data used in the work were obtained previously in previous works of the authors.

2. Basic principles of the model of smeared magnetostructural phase transitions for solid solutions of the $Mn_{1-x}Cr_xNiGe$ system

We proceed from the assumption [8–9] that $Mn_{1-x}Cr_xNiGe$ solid solutions in the temperature range of the structural paramagnetic transition $PMhex(P6_3/mmc) \leftrightarrow PMorth(Pnma)$ are a heterogeneous system consisting of two chaotically distributed regions, each of which is one of two homogeneous phases. Each homogeneous region is considered as a nucleus of the corresponding phase: orthorhombic phase 1 with symmetry group $Pnma$ (further — $orth(Pnma)$) or hexagonal phase 2 with symmetry group $P6_3/mmc$ (further — $hex(P6_3/mmc)$). The thermodynamic potential of such a heterogeneous system, consisting of a mixture of phases 1 and 2, can be represented in the form [3–4]:

$$\Omega = L_1U_1 + L_2U_2 + \tilde{U}_{12}L_1L_2 - TS(L_1, L_2), \quad (1a)$$

$$S(L_1, L_2) = -k_B[L_1 \ln L_1 + L_2 \ln L_2], \quad (1b)$$

where the variables L_1, L_2 — relative number of particles; $U_1 \equiv U_1(T)$, $U_2 \equiv U_2(T)$ — their thermodynamic potentials

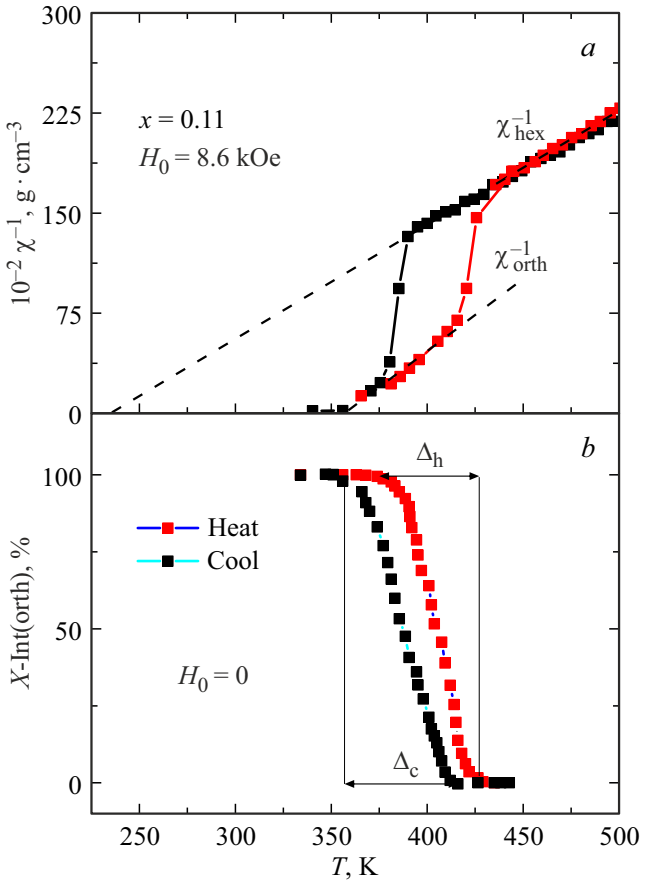

Figure 1. Experimental temperature dependences of the inverse PM susceptibility $\chi^{-1}(T)$ and X-ray intensity $X\text{-Int}_{orth}(T)$, measured in the corresponding fields [1].

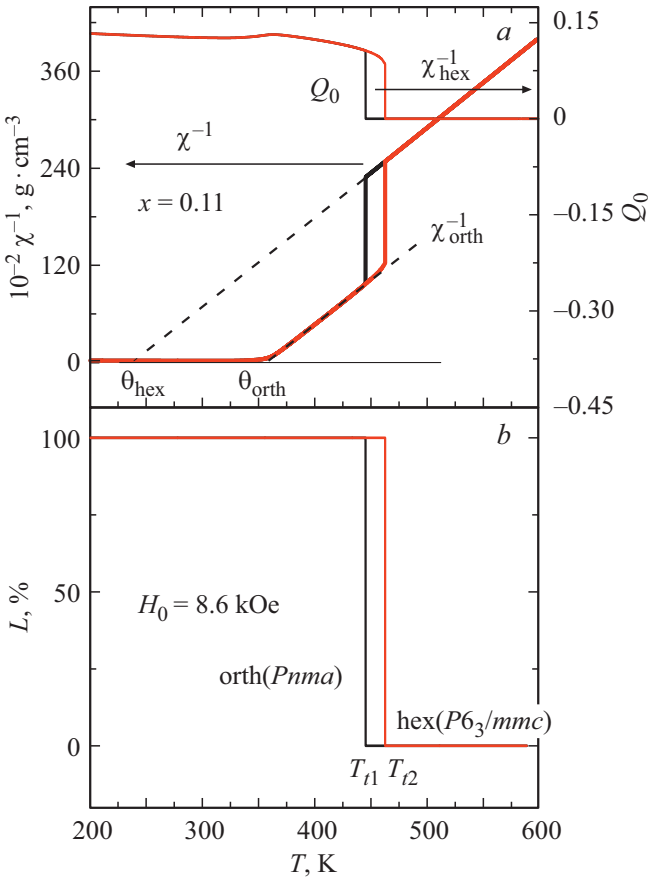

Figure 2. Theoretical temperature dependences of the inverse PM susceptibility and $\chi^{-1}(T)$ phase state function $L(T)$ in the model of the point 1-st order structural phase transition. $Q_0(T)$ — temperature dependence of the structural order parameter describing the point structural transition $hex(P6_3/mmc) \leftrightarrow orth(Pnma)$ in a homogeneous medium [7-8].

in phases 1 and 2, respectively, $S(L_1, L_2)$ — entropy of mixing [4], k_B — Boltzmann constant. $\tilde{U}_{12}$ — interaction potential between the particles.

In the limiting case of non-interacting phases ($\tilde{U}_{12}L_1L_2 \ll 1$), the main driving force for changing the ratio between L_1, L_2 remains the entropy of mixing, which, under the condition $L_1 + L_2 = 1$, can be reduced to the form

$$S = -k_B[L_1 \ln L_1 + L_2 \ln L_2]$$

$$\equiv -k_B[L_1 \ln L_1 + (1 - L_1)\ln(1 - L_1)].$$

Then the formula (1a) takes the form of

$$\Omega = \Delta U_{12}L_1 + U_2 + k_BT[L_1 \ln L_1 + (1 - L_1)\ln(1 - L_1)], \quad (2)$$

where $\Delta U_{12} = U_1 - U_2$.

To determine the phase state function of a heterogeneous system, we minimize the thermodynamic potential according to L_1 ($\partial\Omega/\partial L_1 = 0$) and find the equilibrium value

$$L_1 = \left(1 + e^{\frac{\Delta U_{12}}{k_BT}}\right)^{-1}. \quad (3)$$

We believe that the dependence X-Int$_{\text{orth}}(T)$, which describes the relative change in the content of the orthorhombic phase, can be associated with the temperature dependence of the relative amount of particles $L_1(T)$ of the martensite phase with an orthorhombic structure in the austenitic medium formed by $L_2(T) = 1-L_1(T)$ particles with a hexagonal structure. In the original monograph [3], particles of one phase are defined as nuclei of this phase.

The change in the thermodynamic potential of a particle $\Delta U_{12} \equiv U_2-U_2$ can be represented as a superposition of two components: the bulk $(\tilde{\Omega}_1-\tilde{\Omega}_2)g$, which describes the energy state in the volume of the nucleus, and the surface $(\tilde{\alpha}_1-\tilde{\alpha}_2)g^{2/3}$, which characterizes the energy features of the shape of the nuclei [3,9]:

$$\Delta U_{12} \equiv U_1 - U_2 = (\tilde{\Omega}_1-\tilde{\Omega}_2)g_1 + (\tilde{\alpha}_1-\tilde{\alpha}_2)g_1^{2/3}. \qquad (4)$$

Here $g_1 \approx 50-1000$ — the average number of structural units in a particle [4] (in the case under consideration, the number of initial lattice cells in the volume of a particle of the orthorhombic phase is implied); $\tilde{\Omega}_1, \tilde{\Omega}_2$ — thermodynamic potentials of the nucleus bulk part of the corresponding phases; $\tilde{\alpha}_1, \tilde{\alpha}_2$ — thermodynamic potentials associated with the formation of the surface shape of the nucleus. Here and further we calculate the thermodynamic potentials per lattice cell volume of the initial hexagonal structure.

Expression (4) in structure does not violate the initial condition of conservation of the relative number of particles $L_2 = 1-L_1$, if g_1 is the same for nuclei of both phases: $g_1 = g_2 = g$). Indeed, the left-hand side, by definition, should have the form

$$L_2 = \left(1 + e^{\frac{\Delta U_{21}}{k_B T}}\right)^{-1},$$

where

$$\Delta U_{21} \equiv U_2 - U_1 = (\tilde{\Omega}_2 - \tilde{\Omega}_1)g_2 + (\tilde{\alpha}_2 - \tilde{\alpha}_1)g_2^{2/3}.$$

It is easy to show that the right-hand side of the equality $L_2 = 1-L_1$ with $g_1 = g_2 = g$ has the form

$$1-L_1 = 1-\left(1 + e^{\frac{\Delta U_{12}}{k_B T}}\right)^{-1} = \left(1 + e^{\frac{-(\tilde{\Omega}_1-\tilde{\Omega}_2)g_1-(\tilde{\alpha}_1-\tilde{\alpha}_2)g_1^{2/3}}{k_B T}}\right)^{-1}$$
$$\equiv \left(1 + e^{\frac{\Delta U_{21}}{k_B T}}\right)^{-1}.$$

In the fundamental works on smeared transitions of the 1-st order in shape memory alloys and ferroelectrics [3,5,6,9,10] the microscopic mechanism of the formation of the martensite structure in the nucleus is not reviewed. For example, in [4], where the main attention is paid to describing the mechanism of giant macroscopic deformation of working fluids undergoing a martensitic transformation, the value ΔU_{12} in (3) was approximated by the expression $\Delta U_{12} = B(T-T_C)k_B$. Then

$$L_1(T) = \left(1 + e^{\frac{B(T-T_C)k_B}{T}}\right)^{-1}, \qquad (5)$$

where according to [4] B — the parameter that determines the smearing of the transition in temperature, T_C — the temperature of the transition to the martensite state.

With this approach, the known phenomenological models of point martensitic transformations in Heusler alloys (see, for example, [10–14]) remain out of sight. Meanwhile, the concepts of the order parameter and temperature of the T_C transitions do not coincide in their semantic meaning. Thus, at the description of the smeared transitions [4] the quantity $\eta = L_1-L_2 = 2L-1$ is reviewed as the order parameter η, which varies from -1 to 1. In this case T_C is determined by the condition $L(T_C) = 1/2$.

On the other hand, when considering martensitic transformations, it is often limited to considering point transitions of the 1-st order, which are characteristic of homogeneous systems and occur simultaneously throughout the entire volume of the sample. To describe them, a non-equilibrium thermodynamic potential is used in the form of an expansion in combinations of elastic deformations [10–14]. Two combinations of these deformations e_2, e_3 disappear during the 1-st transition from a tetragonal structure (austenite, $e_2 \neq 0$, $e_1 \neq 0$) to cubic (martensite, $e_2 = e_3 = 0$) and therefore are used as a secondary order parameter. The transition temperature T_C in this case corresponds to the softening temperature of the elastic modulus $a = c_{11}-c_{12} = a_0(T-T_C)$, which determines the 1-st term of the expansion of the non-equilibrium thermodynamic potential in terms of order parameters: $\frac{1}{2}a_0(T-T_C)(e_2^2 + e_3^2)$ [10–14]. In this case, nuclei are implied, but are considered separately, taking into account the model heterogeneity of the system.

In this work, following [8], both approaches to the description of martensitic transformations in the $Mn_{1-x}Cr_xNiGe$ system are taken into account. It is assumed that the appearance of a martensite nucleus (orthophase) with an as yet unknown shape in the crystal lattice occurs when the corresponding transition is stabilized. Point structural PMhex($P6_3/mmc$) $\leftrightarrow$ PMorth($Pnma$) or point magnetostructural PMhex$P6_3/mmc$) $\leftrightarrow$ HMorth($Pnma$) transition with helimagnetic (HM) orthorhombic phase HMorth($Pnma$) as phase 1. Therefore, in (4) the equilibrium expressions of thermodynamic potentials calculated in one or another model of point structural transitions are used as $\tilde{\Omega}_1, \tilde{\Omega}_2$. In particular, when using the exchange-structural model of interacting parameters of the magnetic and structural orders [7–8], which describes point transitions of the 1-st order PMhex($P6_3/mmc$) $\leftrightarrow$ HM,PMorth($Pnma$) in an ideal homogeneous system of $N_0 \gg g$ elementary

$$\tilde{\Omega}_1 = \Omega(\text{orth})/N_0 \equiv \Omega(Q_0, y, e_1, T, P, H)/N_0, \qquad (6a)$$

$$\tilde{\Omega}_2 = \Omega(\text{hex})/N_0 \equiv \Omega(Q_0 = 0, y, e_1, T, P, H)/N_0, \qquad (6b)$$

where Q_0, y — values of equilibrium parameters of the structural and magnetic orders, respectively;

$e_1 \equiv e_1(Q_0, y, P, T)$ — volumetric deformation; $\Omega(Q_0, y, e_1, T, P, H) \equiv \Omega_1$ — equilibrium thermodynamic potential calculated for the rhombic magnetically ordered $y \neq 0$ (paramagnetic $y = 0$) state; similarly $\Omega(Q_0 = 0, y, e_1, T, P, H) \equiv \Omega_2$ — equilibrium thermodynamic potential calculated for the hexagonal magnetic-ordered $y \neq 0$ (paramagnetic $y = 0$) state (P4).

The value $(\tilde{\alpha}_1 - \tilde{\alpha}_2)g^{2/3}$ describing the influence of the surface shape of the nuclei — an as yet unknown function of temperature and pressure. We assume that this term in (4) allows to determine the initial conditions of the $L_1(T)$ dependence during cooling and heating of a heterogeneous system. It is also reasonable to assume that, like the 1-st term in (4), the value $(\tilde{\alpha}_1 - \tilde{\alpha}_2)g^{2/3}$ should „respond " to changes in external conditions: pressure, temperature, magnetic field. In the simplest version, $(\tilde{\alpha}_1 - \tilde{\alpha}_2)g^{2/3}$ is approximated by the expressions

$$(\tilde{\alpha}_1 - \tilde{\alpha}_2)g^{2/3} = g^{2/3}\Delta\alpha_{12}(\Omega_1, \Omega_2) \equiv g^{2/3}(n_1^{c,h}\Omega_1 - n_2^{c,h}\Omega_2), \quad (7)$$

where the numbers $|n_{1,2}^{c,h}| \ll 1$ — model parameters that determine the adjustment of the dependence $L_1(T) \equiv L_{1c}(T)$ during cooling $(n_{1,2}^{c})$ and $L_1(T) \equiv L_{1h}(T)$ during heating $(n_{1,2}^{h})$ of the heterogeneous system. Meanwhile, the values of the once chosen numbers $n_{1,2}^{c,h}$ and g are assumed to be independent of pressure and magnetic field.

The final expressions for the temperature dependences $L_{1c,h}(T)$ at fixed pressure P and magnetic field H, according to (6) have the form

$$L_{1c}(T) = \left(1 + e^{\frac{[\Omega_1 - \Omega_2]g + [n_1^c\Omega_1 - n_2^c\Omega_2]g^{2/3}}{a_2 T}}\right)^{-1} \equiv L_{1c}(T, P, H), \quad (8a)$$

$$L_{1h}(T) = \left(1 + e^{\frac{[\Omega_1 - \Omega_2]g + [n_1^h\Omega_1 - n_2^h\Omega_2]g^{2/3}}{a_2 T}}\right)^{-1} \equiv L_{1h}(T, P, H), \quad (8b)$$

where $a_2 = k_B N_0$, N_0 — number of lattice cells per unit volume (cm^3) (see Appendix).

Magnetic

$$y = \langle \mathbf{U}_n^k \hat{\mathbf{s}}_n^k \rangle / s \equiv \langle \hat{m} \rangle / s = Sp\hat{m}\, e^{\beta h\hat{m}} / sSpe^{\beta h\hat{m}}$$

and structural

$$Q_0 = \langle Q_n \rangle_\rho \equiv \int_{-\infty}^{\infty} \rho_{dso} Q_n dQ_n$$

order parameters for describing point transitions are determined in the $h\mathbf{U}_n^k$ mean field approximation for the spin subsystem and in the biased harmonic oscillator approximation for the structural subsystem

$$\rho_{dso} \equiv \rho_{dso}(Q_n) = \frac{1}{\sqrt{2\pi\tilde{\sigma}}} \exp\left[-\frac{(Q_n - Q_0)^2}{2\tilde{\sigma}}\right]$$

(see Appendix). In the model of smeared transitions, their equilibrium values calculated from the equations of state (P2) are transformed to y^*, Q_0^* (9)

$$y_{c,h}^*(T) = y(T)L_{1c,h}(T), \quad (9a)$$

$$Q_{0c,h}^*(T) = Q_0(T)L_{1c,h}(T). \quad (9b)$$

Accordingly, thermodynamic functions from the variables y and Q_0 transform into functions from y^* and Q_0^*. For instance, temperature dependence $S(T, H, P) \equiv S[Q_0(T), y(T, H), T, H, P]$ of the entropy in the point description (P2) goes into the dependence $S[Q_0^*(T), y^*(T, H), T, H, P]$. Temperature dependences of the inverse PM susceptibility in the region of temperatures of the paramagnetic structural transition $\mathrm{PMhex}(P6_3/mmc) \leftrightarrow \mathrm{PMorth}(Pnma)$ [7] is transformed according to the scheme

$$\chi_{c,h}^{-1}(T) \equiv \chi_{c,h}^{-1}[Q_{0c,h}(T), T] \rightarrow (\chi_{c,h}^*)^{-1}[Q_{0c,h}^*(T), T]$$

at $H = y = 0$ and

$$\chi_{c,h}^{-1}(T) \equiv \chi_{c,h}^{-1}[y_{c,h}(T, H)] = \frac{H_0}{M[y_{c,h}(T, H)]} \rightarrow \frac{H_0}{M[y_{c,h}^*(T, H)]}$$

at $H = H_0$. Here and below, the lower indices c and h — correspond to cooling and heating, $M[y_{c,h}(T, H)]$ correspond to the theoretical values of the specific magnetization during cooling and heating of the sample.

3. Interpretation of the features of the magnetostructural and magnetocaloric properties of samples of the $Mn_{1-x}Cr_xNiGe$ with $0.11 \leq x \leq 0.25$ in the model of smeared transitions

Three types of characteristic features of magnetostructural properties can be distinguished in the $Mn_{1-x}Cr_xNiGe$ system. The properties of the sample with $x = 0.11$ (Figure 3, *a, b, c*) are typical for solid solutions with a Cr concentration within the $0 \leq x < 0.18$ range. The anomalous behavior of the inverse paramagnetic susceptibility and the change in phase state ending below the paramagnetic Curie temperature θ_{orth} (Figure 3, *a, b*) are characteristic of a smeared structural transition of the 1-st order $\mathrm{hex}(P6_3/mmc) \leftrightarrow \mathrm{orth}(Pnma)$, preceding magnetic ordering, Figure 3, *c*. The latter is realized as an isostructural transition2-nd order, $\mathrm{PMorth}(Pnma) - \mathrm{HMorth}(Pnma)$ and stabilizes the simple helimagnetic phase (HM) with the wave vector $\mathbf{q} = [0, 0, q_a]$ [15]. This transition is not smeared, since it occurs in the temperature region of stability of the orthorhombic phase for the entire $(L_{1c,h}(T) \equiv 1)$ crystal. The properties of the sample with $x = 0.18$ are determined by the so-called reversible transitions [16], which are accompanied by temperature hysteresis and have different magnetization slopes with an initial decrease and subsequent increase of temperature (Figure 4, *c*). Here, a sharp decrease of the inverse susceptibility χ_c^{-1} (Figure 3, *c*) and magnetization (Figure 4, *c*) coincides with an increase

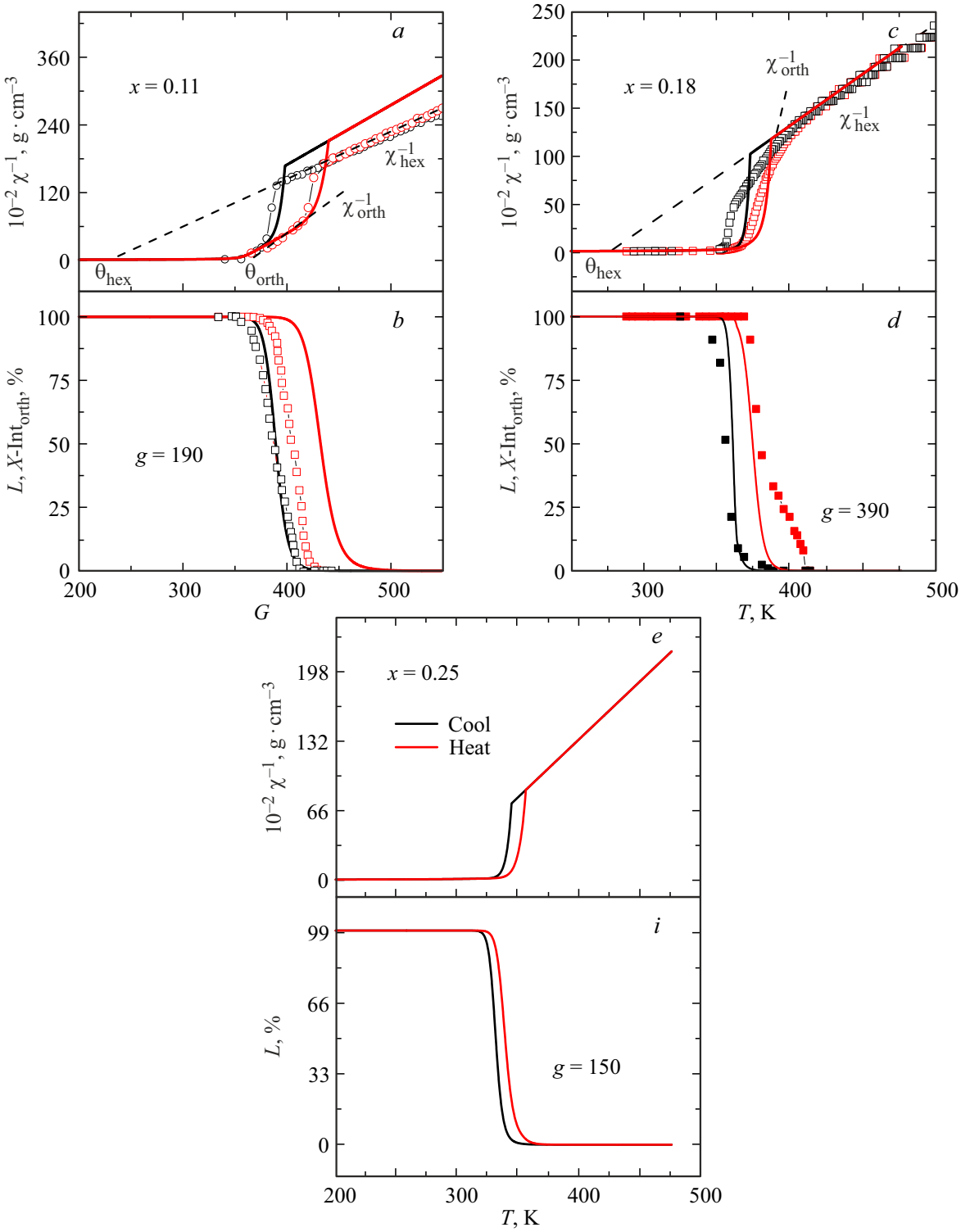

Figure 3. Combined experimental (symbols) and theoretical (lines) temperature dependences of the magnetostructural characteristics of a number of alloys of the $Mn_{1-x}Cr_xNiGe$ system at atmospheric pressure. g-number of structural units in a orthorhombic nucleus; experimental dependences taken from [1].

of the content of the orthorhombic phase $L_{1c}(T)$, X-Int (T) (Figure 3, d). Such behavior can be interpreted according to [16] as the occurrence of a magnetostructural transition of the 1-st order PMhex$(P6_3/mmc) \leftrightarrow$ FMorth$(Pnma)$) upon an initial decrease of temperature. This transition will be smeared, since it is located in the area of the greatest change $L_{1c}(T)$, X-Int$_{\text{orth}}(T)$ (Figure 3, d). A non-smeared isostructural transition of the 2-nd order

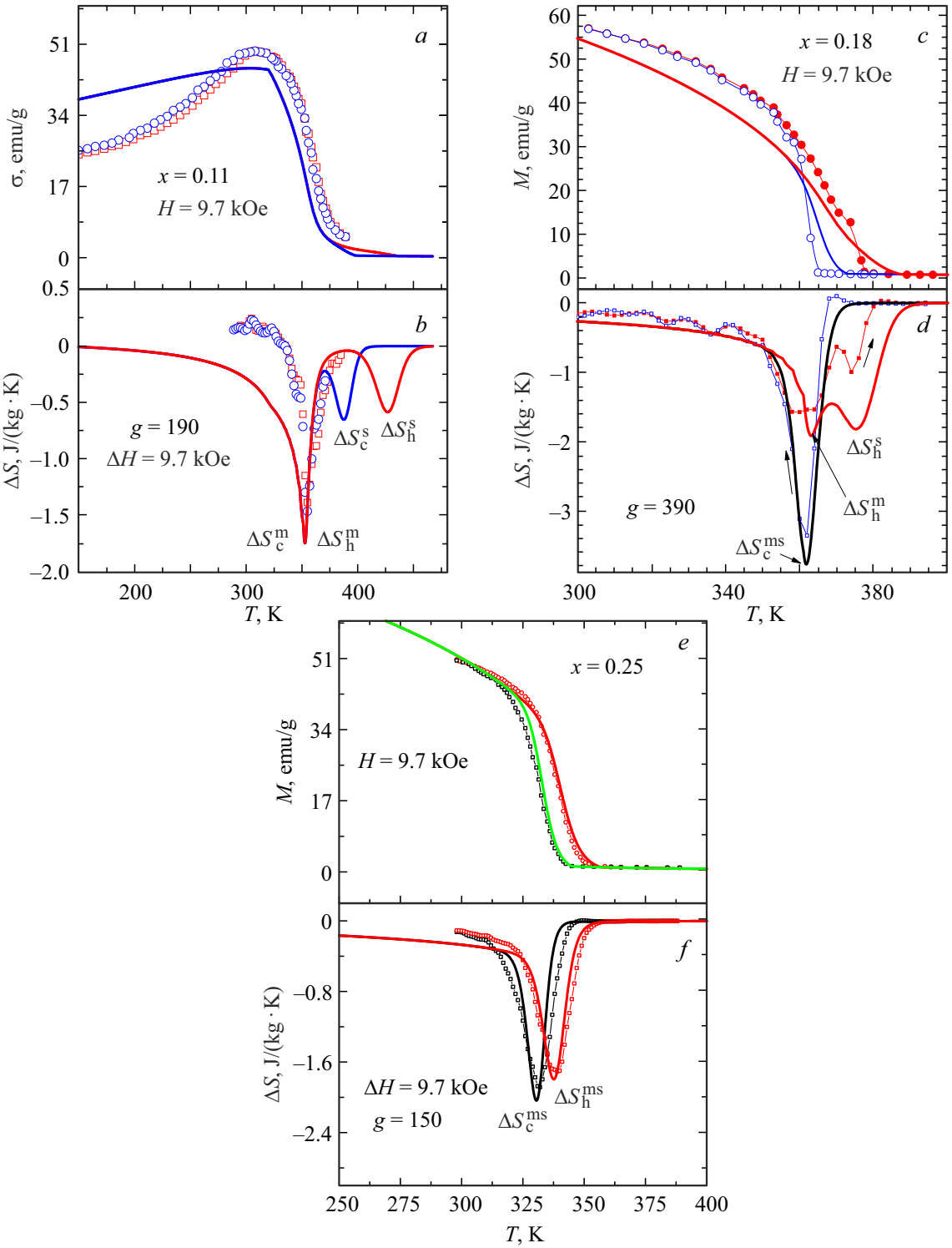

Figure 4. Comparison of temperature dependences of magnetic $M(T)$ and magnetocaloric $\Delta S(T)$ characteristics for a number of samples of the $Mn_{1-x}Cr_xNiGe$ system. Symbols — experimental data from [19,16,19] respectively; lines — model.

FMorth($Pnma$)−PMorth($Pnma$)) is observed in case of an inverse increase of temperature within the rhombic phase (its beginning and end at a temperature lower than the main change in the function $L_{1h}(T)$, X-Int$_{oth}(T)$ Figure 3, *d*). Here and below, the upper index „*“ used in (9) to denote the parameters of smeared transitions is not used. Therefore, the characteristics of point transitions are highlighted in text. In the sample with $x = 0.25$, ferromagnetic ordering (disordering) is realized as a1-st order transition both with increasing and decreasing temperature [18–19].

This transition is accompanied by temperature hysteresis and a relatively sharp change in magnetization, followed by an almost hysteresis-free and smooth increase at low temperatures (Figure 4, *e*).

Experimental isothermal dependences of entropy $\Delta S(T)$, calculated on the basis of Maxwell's relation in the range of magnetic field variations $\Delta H = 9.7\,\text{kOe}$, complement the magnetostructural features of the samples under study. Figure 4 compares the experimental and theoretical dependences of the specific $M(T)$, and $\Delta S(T)$, which give an idea of the relationship between the magnetic and magnetocaloric features of the $Mn_{1-x}Cr_xNiGe$ system at atmospheric pressure. Theoretical dependences $\Delta S(T)$ were calculated according to the scheme

$$\Delta S(T) = S[Q_0(T), y(T, H), T, H, P] - S[Q_0(T), y(T, 0), T, 0, P]. \quad (10)$$

As can be seen from Figure 4, *a, b*, alloys with separated structural and magnetic transitions are characterized by a four-peak structure of the $\Delta S(T)$ dependence (2 peaks during cooling: structural$\Delta S_c^s(T)$ and magnetic $\Delta S_c^m(T)$; 2 peaks during heating: $\Delta S_h^s(T)$ and $\Delta S_h^m(T)$ structural and magnetic, respectively). According to the model, the first two combined low-temperature peaks $\Delta S_h^m(T)$ and $\Delta S_c^m(T)$ correspond to the magnetocaloric contribution from the isostructural magnetic phase transition $\text{PMorth}(Pnma)-\text{HMorth}(Pnma)$ within the orthorhombic phase. The appearance (disappearance) of this phase as a result of a smeared structural transition of the 1-st order $\text{PMhex}(P6_3/mmc) \leftrightarrow \text{PMorth}(Pnma)$) may be the cause of two high-temperature peaks $\Delta S(T)$, corresponding to the cooling of $\Delta S_c^s(T)$ and heating of $\Delta S_h^s(T)$. These „structural" peaks are significantly smaller in absolute value than the isostructural „magnetic" peaks $\Delta S_h^m(T)$, $\Delta S_c^m(T)$. There are no experimental points for the dependences $\Delta S_h^s(T)$, $\Delta S_c^s(T)$ in Figure 4, *b*. However, their existence is indirectly confirmed by DTA analysis in work [17].

There is a slightly different feature for the central sample $x = 0.18$. Here, the three-peak structure reflects the asymmetric combination of structural and magnetic transitions. A sharp, large, low-temperature peak is a superposition of magnetic and structural contributions. This peak $\Delta S_c^{ms}(T)$ characterizes a smeared magnetostructural transition of the 1-st order $\text{PMhex}(P6_3/mmc) \leftrightarrow \text{FMorth}(Pnma)$), which occurs when the sample is cooled. When the sample is heated, a sequence of two phase transitions occurs. The first isostructural transition of the 2-nd order $\text{FMorth}(Pnma) \rightarrow \text{PMorth}(Pnma)$ corresponds to the magnetic peak $\Delta S_h^m(T)$. The second smeared structural transition of the 1-st order. $\text{PMorth}(Pnma) \rightarrow \text{PMhex}(P6_3/mmc)$ corresponds to the structural peak $\Delta S_h^s(T)$. The structural and magnetic transitions are combined for $x = 0.25$ during cooling and heating as well. The dual-peak structure $\Delta S(T)$ is implemented. Each peak of which relates to the cooling $\Delta S_c^{ms}(T)$ and heating $\Delta S_h^{ms}(T)$ of the sample, which, during cooling and heating, experiences smeared magnetic structural (ms) transitions of the 1-st order $\text{PMhex}(P6_3/mmc) \rightarrow \text{FMorth}(Pnma)$, $\text{FMorth}(Pnma) \rightarrow \text{PMhex}(P6_3/mmc)$, respectively. That is, each peak corresponds to a superposition of diffuse magnetic and structural transitions of the 1-st order. These conclusions are confirmed by a combination of theoretical magnetic, caloric and structural characteristics shown in Figure 5.

In Figure 5, the structural characteristics include dimensionless parameters of local structural order Q_0, (see Appendix). As can be seen from Figure 5, *a, b* the temperature region of change in the magnetic order parameter $y_{c,h}^0 \equiv y_{\text{cooling,heating}}^{H=0}$ is in the stability region of the orthorhombic phase, which lies beyond the high-temperature change in the structural order parameter Q_0. Therefore, the low-temperature peaks $\Delta S_h^m(T)$, $\Delta S_c^m(T)$ correspond only to the magnetic contribution enhanced by the isostructural transition of the 2-nd order $\text{PMorth}(Pnma) \leftrightarrow \text{HMorth}(Pnma)$ in the already stable orthorhombic phase ($Q_0/Q_{0\,\max} \approx 1$). High-temperature peaks are located precisely in the region of temperature changes in the structural order parameter above the Neel temperature T_N, i.e., outside the main change in both the magnetic order parameter $y(H = 0)$ and magnetization $M(H) = M_0 y(H)$. For the case of $x = 0.18$ (Figure 5, *c, d*) the combination of structural and magnetic transitions occurs with the decrease of the temperature (curves Q_{0c} and M_c^H increase in the same temperature range). This results in the occurrence of the magnetostructural transition $\text{PMhex}(P6_3/mmc) \leftrightarrow \text{FMorth}(Pnma)$ and the appearance of a single maximum peak as a result of the positive combination of structural and magnetic contributions in $\Delta S(T)$. The smeariness of the structural transition imposes its own characteristics on the magnetocaloric and magnetostructural properties, but does not change the main reason for the positivity of the structural and magnetic contributions — a decrease of structural and magnetic symmetries with a strong relationship between the parameters of the magnetic and structural orders (see Appendix). As the temperature increases, the temperature intervals of changes in the parameters of the structural and magnetic orders in a magnetic field (curves Q_{0h} and M_h^H) do not coincide. Therefore, as in the case of $x = 0.11$, a sequence of two transitions is observed: an isostructural magnetic phase transition of the 2-nd order $\text{FMorth}(Pnma)-\text{PMorth}(Pnma)$ and a smeared paramagnetic structural transition of the 1-st order $\text{PMorth}(Pnma) \rightarrow \text{PMhex}(P6_3/mmc)$. The magnetic and structural peaks are separated and are significantly inferior in absolute value to the single magnetostructural peak.

For $x = 0.25$, the initial parameters of the semimicroscopic Hamiltonians (see Appendix) are selected in such a way that in the used model of diffuse transitions, a magnetostructural transition of the 1-st order $\text{PMhex}(P6_3/mmc) \leftrightarrow \text{FMorth}(Pnma)$ is realized with decreasing and increasing temperature. It should be noted that the results of the point model and the smeared

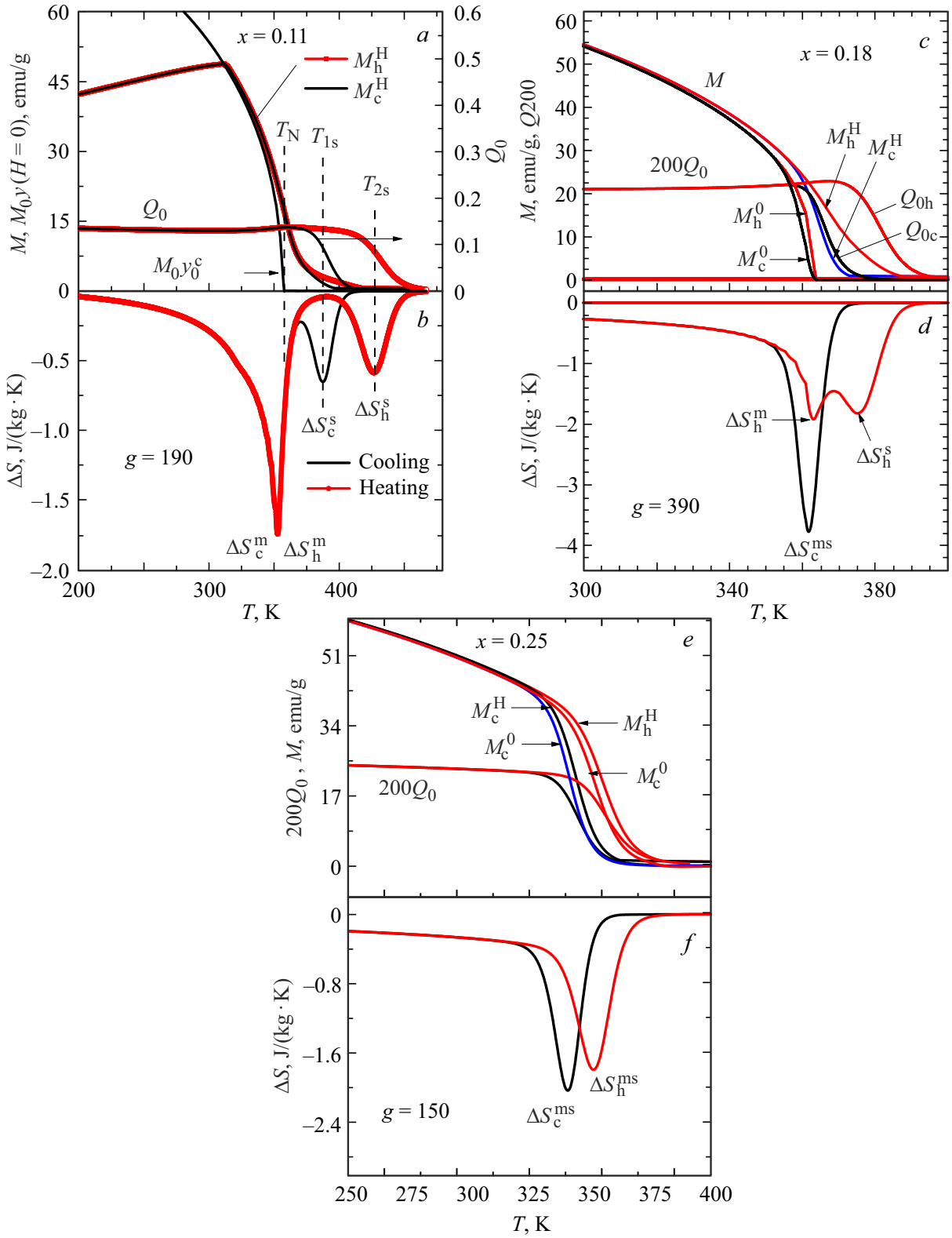

Figure 5. Relationship between the peak structure of $\Delta S(T)$ and magnetocaloric and magnetostructural characteristics (theory). The calculated dependences were carried out using the maximum magnetic field $H = 9.7$ kOe. Temperatures T_N — Neel temperature; T_{1s}, T_{2s} — temperatures associated with the temperatures of appearance and disappearance of the structural order parameter Q_0 as a result of a smeared paramagnetic structural transition of the 1-st order PMhex($P6_3/mmc$) ↔ PMorth($Pnma$).

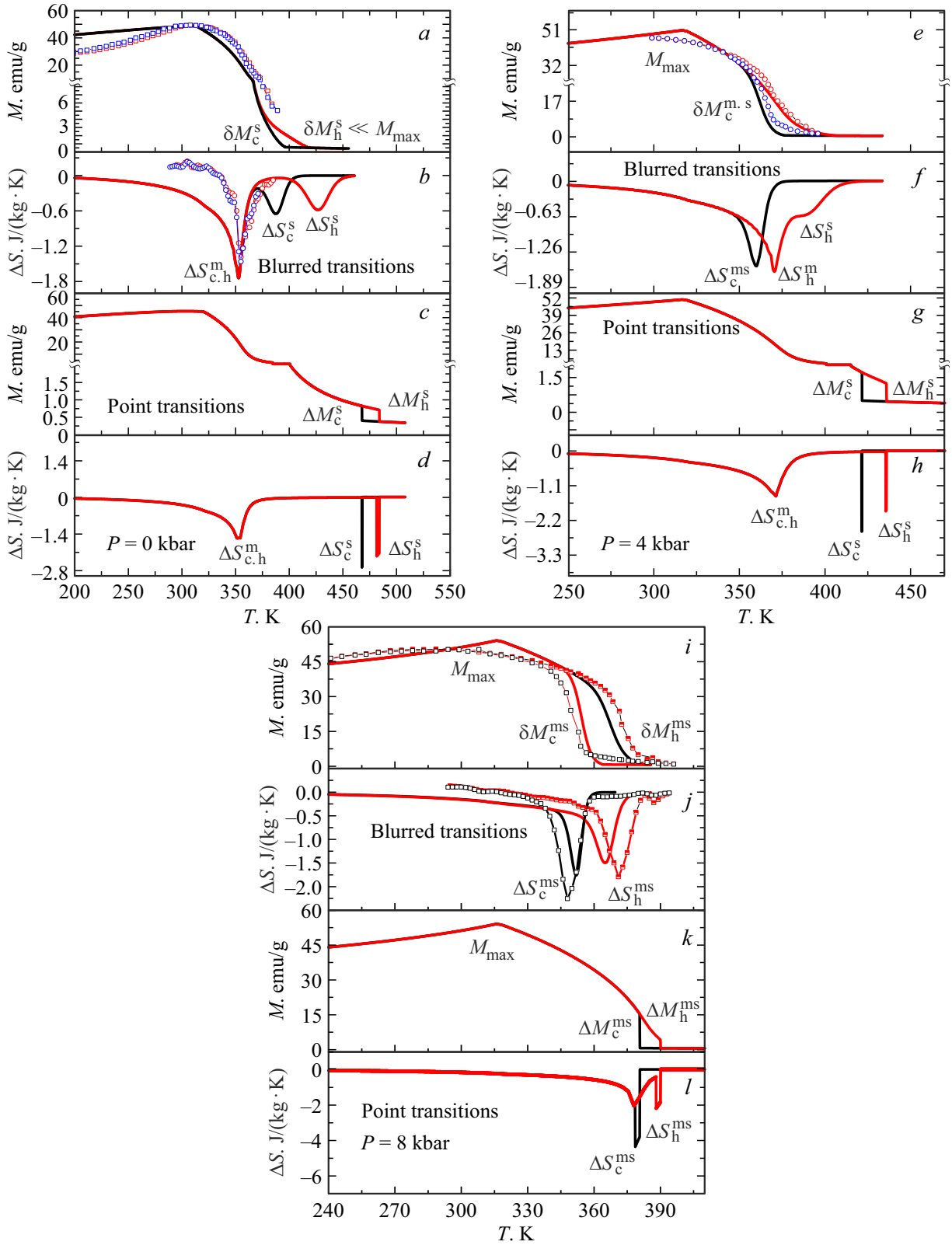

Figure 6. Peculiarities of pressure transformation of magnetostructural states in the model of smeared and point transitions of the 1-th order for a sample with $x = 0.11$. Symbols — experiment, lines — theory.

transition model may have significant qualitative differences in this case, and not only in the absence of stepwise magnetostructural characteristics.

As can be seen from Figure 5, *e, f*, the two-peak structure of $\Delta S(T)$ here can be quite reasonably associated with the coincidence of temperature intervals of changes in the magnetic and structural order parameters. Let us note that, unlike the previous cases, the lines in the pairs M_c^H, M_c^0 and M_h^H, M_h^0 show the displacement of the entire transition. This means that smeared magnetostructural transitions of the 1-st order, like point transitions, can describe transitions of the1-st order induced by a magnetic field.

Another peculiarity of the system properties is the pressure transformation of the magnetostructural properties. Using the example of a sample with $x = 0.11$, as part of the smeared transition model, we will review a series of stages of increasing pressure to 8 kbar. From Figure 6 it is clear that at $p = 4$ kbar a state with a reverse 1-st order transition and a three-peak structure $\Delta S(T)$ arises. This magnetocaloric state of the helimagnetic phase is similar to the magnetocaloric ferromagnetic state in the sample with $x = 0.18$ at atmospheric pressure.

At $p = 8$ kbar, the magnetostructural state characteristic of a sample with $x = 0.25$ at $p = 0$ is reproduced: with a decrease (increase) in temperature, a smeared magnetostructural transition of the 1-st orderPMhex$(P6_3/mmc) \leftrightarrow$ FMorth$(Pnma)$ is realized, with a two-peak structure $\Delta S(T)$. At the same time, relatively sharp (but not abrupt) changes in magnetization in $\delta M_{c,h}^{ms}$ temperature region of the smeared magnetostructural transition of the 1-st order PMhex$(P6_3/mmc) \leftrightarrow$ FMorth$(Pnma)$ are of the same order of magnitude as its maximum value $M_{\max}$.

It should be noted that for a sample with $x = 0.11$, the helimagnetic phase HMorth$(Pnma)$) is weakly resistant to the influence of an external magnetic field. In a magnetic field, the dependence has a maximum and signs of the helimagnetic state begin to appear only below the temperature of maximum magnetization. Therefore, in a magnetic field of the order of 1T for a number of helimagnetic samples, we can talk about magnetostructural PMhex$(P6_3/mmc) \leftrightarrow$ FMorth$(Pnma)$, or isostructural PMorth$(Pnma)-$FMorth$(Pnma)$ transitions from a magnetized paramagnetic to a ferromagnetic state. These theoretical results are confirmed by pressure experimental studies in [7,16–18].

It is of interest to compare the results of the model of smeared and point transitions (Figure 6). As can be seen from Figure 6, *d, h, l*, along with the quantitative discrepancy in the $|\Delta S(T)|$ values, a qualitative discrepancy in the type of transitions also arises. In the point model, at $p = 4$ kbar, the four-peak structure $\Delta S(T)$, characteristic of temperature-separated structural transitions of the 1-st order PMhex$(P6_3/mmc) \leftrightarrow$ PMorth$(Pnma)$ and magnetic isostructural transitions of the 2-nd order PMorth$(Pnma)-$HMorth$(Pnma)$, is preserved as at $p = 0$ (Figure 6, *h*). A 1-st order magnetostructural transition PMhex$(P6_3/mmc) \leftrightarrow$ HMorth$(Pnma)$ is realized as the temperature decreases, with which one magnetostructural peak ΔS_c^{ms} is associated In the model of smeared transitions at this pressure (Figure 6, *f*). Upon subsequent heating, a chain of transitions of the 2-nd and 1-st orders HMorth$(Pnma) \rightarrow$ PMorth$(Pnma) \rightarrow$ PMhex$(P6_3/mmc)$ is realized. These transitions are associated with 2 peaks ΔS_h^m and ΔS_h^s. In total, a three-peak structure appears (Figure 6, *f*), characteristic of reversible magnetostructural transitions of the 1-st order.

4. Conclusion

The analysis of the results obtained allows to state the following.

1. In the proposed approach, the transition from point structural transitions of the 1-st order to smeared ones is carried out by transformation from a step function of the phase state to a diffuse function $L(T)$ of the relative number of nuclei of the orthorhombic phase and subsequent transformation of the order parameters according to the obvious scheme.

2. The temperature range of smearing of thermodynamic functions is determined by the number of structural units g in the nucleus of the rhombic phase 1 and the relationship between the lability temperatures of the order parameters and the temperature of equality of the thermodynamic potentials of the rhombic (Ω_1) and hexagonal (Ω_2) phases in a point approximation.

3. Hysteresis phenomena during cooling (c) and heating (h) are determined by the relationship between the energies of the bulk part of the nucleus $(\Omega_1-\Omega_2)g$, proportional to the value g, and the surface part of the nucleus proportional to $(\Omega_1 n_2^{c,h}-\Omega_2 n_2^{c,h})g^{2/3}$ at $|n_{1,2}^{c,h}| \ll 1$.

4. The increase of the degree of smearing (decrease of the parameter g) results in a decrease of the maximum value of the magnetocaloric effect indicators (value $|\Delta S(T)|$).

5. The smearing of the functions of the $L(T)$ phase state leads to the overlapping of areas of magnetostructural stability separated in the pointwise description P–T and the opportunity of the appearance of qualitatively new states and smeared magnetostructural transitions under the influence of pressure and a magnetic field.

Funding

The work was supported by the Ministry of Education and Science of the Russian Federation, budget topic „Fundamental and Applied Aspects of the Development of the Physics of Magnetic Phenomena in Correlated Systems, FREZ-2023-0002“ (V.I.V., A.V.G., I.F.G., O.E.K.). Assignment 1.2.1 „Synthesis of new magnetic materials that are promising for the development of technical devices of a new generation“ subprogram „Condensed matter physics and the creation of new functional materials and technologies for their production“ (V.I.M.).

Conflict of interest

The authors declare that they have no conflict of interest.

Appendix

The subsequent presentation is based on works [7,8] in which the spin (s) and structural (Q) and elastic (e) subsystems are described by the corresponding microscopic Hamiltonians. The Heisenberg Hamiltonian for the spin subsystem consisting of $N(1-x)$ magnetically active Mn atoms, and the Hamiltonian of independent anharmonic soft modes for the structural subsystem of $N_0 = N/2$ lattice hexagonal cells. The total thermodynamic potential of such a system Ω in the presence of an external magnetic field $\mathbf{H} = [0, 0, H]$ is calculated in the approximation of a spatially periodic mean field $\mathbf{h} = h\mathbf{U}_n^k$ (U_k^n — unit vector) for the spin subsystem and in the approximation of a biased harmonic oscillator (dso) for the structural elastic subsystem. The independent changing variables in this case are the parameters of the magnetic and

$$ys = \langle \mathbf{U}_n^k \hat{\mathbf{s}}_n^k \rangle \equiv \langle \hat{m} \rangle = Sp\hat{m}e^{\beta h\hat{m}}/Spe^{\beta h\hat{m}}$$

structural

$$Q_0 \equiv \langle Q_n \rangle \equiv \int_{-\infty}^{\infty} \rho_{dso} Q_n dQ$$

$$= \int_{-\infty}^{\infty} \frac{1}{\sqrt{2\pi\sigma}} \exp\left[-\frac{(Q_n - Q_0)^2}{2\sigma}\right] Q_n dQ_n$$

orders, dispersion

$$\sigma = \langle [Q_n - Q_0]^2 \rangle \equiv \int_{-\infty}^{\infty} \rho_{dso} [Q_n - Q_0]^2 dQ_n,$$

volumetric e_1 and orthorhombic e_2 deformations.

The equilibrium values of these independent variables as a function of temperature are found from the system of equations of state

$$(\partial\Omega/\partial Q_0) = 0, \quad (\partial\Omega/\partial y) = 0, \quad (\partial\Omega/\partial\sigma) = 0,$$
$$(\partial\Omega/\partial e_1) = 0, \quad (\partial\Omega/\partial e_{21}) = 0. \qquad \text{(A1)}$$

The last three equations have solutions in analytical form. The first two are reduced to the form (A2) and solved numerically.

$$(\partial\Omega/\partial Q_0) = 0, \qquad \text{(A2a)}$$
$$y = B_x(X), \qquad \text{(A2b)}$$

where

$$B_s(X) = \left[\left(\frac{1}{2s+1}\right)\coth\frac{1}{2s+1}X - \left(\frac{1}{2s}\right)\coth\frac{1}{2s}X\right]$$

— Brillouin function

$$z(X) = Spe^{\beta h\hat{m}} \equiv \sum_{m_s=-s}^{s} e^{\beta h m_s}, \; X = hs/k_B T, \; \hat{m}_n^k = \mathbf{U}_n^k \hat{\mathbf{s}}_n^k = \hat{m},$$

m_s — the eigenvalue of the operator of the projection of the spin operator $\hat{\mathbf{s}}_n^k$ onto the direction of the average spatially inhomogeneous field $\mathbf{h} = h\mathbf{U}_n^k$ k-th atom in the n-th lattice cell (structural unit) of the original hexagonal lattice. The dependence of the modulus of the spatially heterogeneous field h on the parameters of the structural order leads to the relationship between the spin and structural subsystems. Therefore

$$X = \equiv X[T, H, P, Q_0(T), y(T)], \; h \equiv h[T, H, P, Q_0(T), y(T)],$$

and their explicit expressions are given in Ref. [7]. The expression for the equilibrium entropy $S = -(\partial\Omega/\partial T)$ and thermodynamic potential Ω as a function of temperature T, pressure P, magnetic field H systems of N_0 structural units per unit volume have the form

$$S(T, P, H) = Nk_B[\ln z(X) - yX] + \frac{\alpha}{\kappa} e_1 + \frac{N_0 k_B}{2}\ln(\sigma), \qquad \text{(A3)}$$

$$\Omega(T, P, H) = N(h - 2\mu_0 \mathbf{H}\mathbf{U}_n^k)ys/2 - k_B NT \ln z(X)$$
$$+ U(Q_0, \sigma) - T\frac{k_B}{2} N_0 \ln\sigma + \Omega_e(e_1, e_2, T, P) \qquad \text{(A4)}$$

$\mathbf{U}_n^k \equiv \mathbf{U}_n^k(\mathbf{q}) = \left[\cos(\mathbf{q}\mathbf{R}_n^k)\sin(\vartheta), \sin(\mathbf{q}\mathbf{R}_n^k)\sin(\vartheta), \cos(\vartheta)\right]$ — unit vector defining the direction of the average field for the atomic spin at position $\mathbf{R}_n^k$ in the presence of a magnetic field $\mathbf{H} = [0, 0, H]$

$$U(Q_0, \sigma) = \frac{\omega^2}{2}(Q_0^2 + \sigma) + \frac{\gamma}{4}(Q_0^4 + 6Q_0^2\sigma + 3\sigma^2)$$
$$+ \frac{\Gamma}{6}(Q_0^6 + 15Q_0^4\sigma + 45Q_0^2\sigma^2 + 15\sigma^3)$$
$$- \frac{1}{2}\nu_0(1 + L_2 e_1 + L_3 e_2)Q_0^2, \qquad \text{(A5)}$$

where the equilibrium variables

$$y \equiv y(T), \quad Q_0 \equiv Q_0(T),$$
$$e_1 \equiv e_1[T, P, Q_0(T), y(T)], \quad e_2 \equiv e_2[Q_0(T)],$$
$$\sigma \equiv \sigma[T, Q_0(T)]$$

are solutions of the equations of state (A1) for given values of pressure and magnetic field.

Where $\omega^2 = N_0\tilde{\omega}^2$, $\gamma = N_0\tilde{\gamma}$, $\Gamma = N_0\tilde{\Gamma}$,

$$N_0 V_0 = N_0 \sum_{n'} V_{nn'} \equiv N_0 V_0(e_1, e_2) = \nu_0(1 + L_2 e_1 + L_3 e_2).$$

The expression of thermodynamic potentials in the orthorhombic Ω_1 and hexagonal Ω_2 phases is determined from (A4) as

$$\Omega_1 \equiv \Omega\big(Q_0(T), y(T), T, H, P\big)$$

and

$$\Omega_2 \equiv \Omega\big(0, y(T), T, H, P\big).$$

References

[1] V.I. Val'kov, V.I. Kamenev, V.I. Mitsiuk, I.F. Gribanov, A.V. Golovchan, T.Yu. Delikatnaya. FTT **59**, 266 (2017). (in Russian).
[2] S.V. Vonsovsky. Magnetizm. Nauka, M. (1971). 1032 p. (in Russian).
[3] B.N. Rolov, V.E. Yurkevitch. Fizika razmytykh fazovykh perekhodov. Izd-vo Postovsk. un-ta, R/na-Donu. (1983). 320 s. (in Russian).
[4] A. Malygin. UFN **71**, *1*, 187 (2001). (in Russian).
[5] A.A. Bokov. Ferroelectrics **183**, 65 (1996).
[6] A.A. Bokov. ZhETF **111**, *5*, 1817 (1997). (in Russian).
[7] V.I. Val'kov, I.F. Gribanov, E.P. Andreychenko, O.E. Kovalev, V.I. Mitsiuk. FTT **65**, *10*, 1758 (2023). (in Russian).
[8] V.I. Val'kov, A.V. Golovchan, O.E. Kovalev, N.Yu. Nirkov. FTVD **33**, *4*, 36 (2023). (in Russian).
[9] Ya.I. Frenkel'. Statistical physics. Publisher AS USSR, M.-L. (1948). 760 s. (in Russian).
[10] L.S. Metlov, V.V. Koledov, V.G. Shavrov. FTVD **28**, *1*, 46 (2018). (in Russian).
[11] L.S. Metlov, V.D. Poimanov. FTVD **28**, *1*, 62 (2018). (in Russian).
[12] L.S. Metlov. FTVD **29**, *1*, 28 (2019). (in Russian).
[13] L.S. Metlov, A.G. Petrenko. FTVD **28**, *3*, 46 (2018). (in Russian).
[14] L.S. Metlov, V.V. Koledov, V.G. Shavrov, Yu.D. Zavorotnev, Yu.V. Tehtelev. FTVD **30**, *2*, 56 (2020). (in Russian).
[15] B. Penca, A. Hoserb, S. Barana, A. Szytutaa. Phase Transit. **91**, *2*, 118 (2018).
[16] V.I. Val'kov, V.I. Kamenev, A.V. Golovchan, I.F. Gribanov, V.V. Koledov, V.G. Shavrov, V.I. Mitsiuk, P. Duda. FTT *63*, *5*, 628 (2021). (in Russian).
[17] A. Szytuta, S. Baran, T. Jaworska-Gota, M. Marzec, A. Deptuch, Yu. Tyvanchuk, B. Penc, A. Hoser, A. Sivachenko, V. Val'kov, V. Dyakonov, H. Szymczak. J. Alloys Comp. **726**, 978 (2017).
[18] V.I. Valkov, A.V. Golovchan, I.F. Gribanov, E.P. Andreychenko, O.E. Kovalev, V.I. Mitsiuk, A.V. Mashirov. FMM **124**, *11*, 1044 (2023). (In Russian).
[19] I.F. Gribanov, V.V. Burkhovetsky, V.I. Val'kov, A.V. Golovchan, V.D. Zaporozhets, V.I. Kamenev. T.S. Sivachenko. FTVD **30**, *1*, 83 (2020). (in Russian).

Translated by A.Akhtyamov